RGNZ/MGPB

Pedogenesis of Lateritic Soils and the Enrichment of Critical Metals: A Study from Southeast Sulawesi, Indonesia

Khalil Ibrahim[1]; Satria Bijaksana[2]*; Ulvienin Harlianti[3]; Putu Billy Suryanata[4], La Ode Ngkoimani[5], Suryawan Asfar[6], Silvia Jannatul Fajar[7]

[1] *Faculty of Mining and Petroleum Engineering, Institut Teknologi Bandung, Jalan Ganesa 10, Bandung 40132, Indonesia.*
https://orcid.org/0000-0002-7108-5457

[2] *Faculty of Mining and Petroleum Engineering, Institut Teknologi Bandung, Jalan Ganesa 10, Bandung 40132, Indonesia.*
https://orcid.org/0000-0001-6374-4128

[3] *Faculty of Mining and Petroleum Engineering, Institut Teknologi Bandung, Jalan Ganesa 10, Bandung 40132, Indonesia.*
https://orcid.org/0000-0002-4867-1191

[4] *Faculty of Mining and Petroleum Engineering, Institut Teknologi Bandung, Jalan Ganesa 10, Bandung 40132, Indonesia.*
https://orcid.org/0000-0001-6701-2311

[5] *Faculty of Earth Sciences and Technology, Universitas Halu Oleo, Kampus Hijau Bumi Tridharma, Kendari 93232, Indonesia,*
https://orcid.org/ 0000-0001-9076-9355

[6] *Faculty of Earth Sciences and Technology, Universitas Halu Oleo, Kampus Hijau Bumi Tridharma, Kendari 93232, Indonesia,*
https://orcid.org/0000-0002-8207-1210

[7] *Faculty of Mining and Petroleum Engineering, Institut Teknologi Bandung, Jalan Ganesa 10, Bandung 40132, Indonesia.*
https://orcid.org/0000-0002-9499-2092

Abstract

Lateritic soil is a prospective source of metals termed critical or strategic metals due to their use in high-technology industries. Critical metals include rare earth elements (REEs). In this study, two profiles of lateritic outcrops from the Ni-producing area of Southeast Sulawesi in Indonesia were sampled for magnetic susceptibility as well μ-XRF analyses to identify how the concentration of critical metals changed during pedogenesis. The results show that there are three different patterns from the bottom layer up. The first pattern is enrichment experienced by Sc, La, Cr, and Ti. The second pattern is depletion experienced by Ni, Nd, and Ho. The third pattern is the localization of high concentration at a certain depth, as experienced by Co, Ce, and V. The concentration of certain critical metals correlates either positively or negatively with magnetic susceptibility, inferring that magnetic susceptibility might be used as a proxy indicator for critical metal concentration in lateritic soil.

Keywords:

critical metals; lateritic soil; pedogenesis; magnetic susceptibility; Southeast Sulawesi.

1. Introduction

Certain metals, including rare earth elements (REEs), platinum group metals (PGM), indium (In), tungsten (W), tin (Sn), niobium (Nb), thallium (Tl), gallium (Ga), and magnesium (Mg), are termed critical metals due to their high demands and market values (**Olivetti et al., 2017**; **Hayes and McCullough, 2018**; **Ulrich et al., 2019**; **Watari et al., 2020**). They are highly valued for technological applications, such as super magnet technology, advanced electronics, lighting, and serving as the world's biggest export commodity (**Goodenough et al., 2016; Balaram, 2019; 2022; Botelho Junior et al., 2021**; **Ilankoon et al., 2022; Stratiotou Efstratiadis and Michailidis, 2022**). Critical metals, especially REEs, and other strategic minerals can be found in either

primary or secondary deposits (**Balaram, 2019; 2022; Batapola et al., 2020**). The presence of critical metals, including REEs, in secondary deposits such as lateritic deposits has been reported in deposits such as those in New Caledonia (**Teitler et al., 2019; Ulrich et al., 2019**); Madagascar (**Berger et al., 2014**); Brazil (**Putzolu et al., 2021**); Australia (**Chassé et al., 2017; Putzolu et al., 2019**); the Dominican Republic (**Aiglsperger et al., 2016**); and the Philippines (**Gibaga et al., 2022**). In Indonesia, the presence of REEs has also been reported in lateritic soil as a by-product of nickel mining (**Maulana et al., 2016; PSDMBP, 2019**). Laterization itself is a pedogenic process common in soils found in tropical and subtropical environments (**Safiuddin et al., 2011**; **Ananthapadmanabha et al., 2014**). In turn, the weathering of mafic and ultramafic rocks in tropical regions is affected by rainfall, elevation, and temperature (**Farrokhpay et al., 2019**; **Hamdan et al., 2020**; **Choi et al., 2021**).

Corresponding author: Satria Bijaksana
e-mail address: satria@fi.itb.ac.id
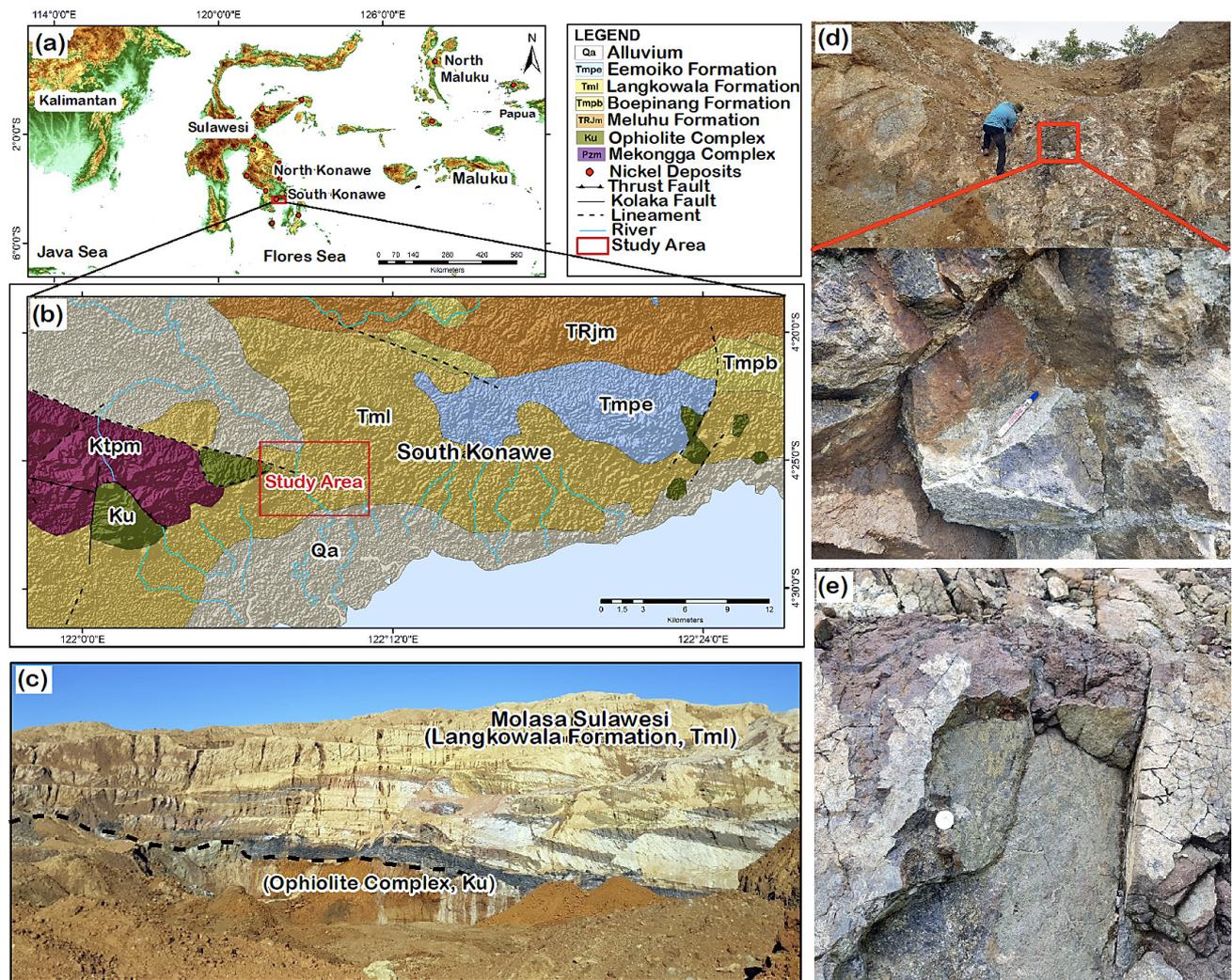
Figure 1: (a) Simplified geological map of Sulawesi Island and its surroundings showing the potential for nickel laterite; (b) regional geological map of the study area (modified from **Simandjuntak et al., 2011**); (c) typical lateritic outcrop in the study area; (d) peridotites that were found in the study area; and (e) serpentinites that were found in the surrounding study area

The differentiation of REE contents in lateritic soils and its relationship with pedogenesis, however, are not known with certainty, as research on these matters is rather limited. In this study, we examine the REEs content of lateritic soil outcrops in nickel mines in the Indonesian province of Southeast Sulawesi (see **Figure 1a**). This province is one of the top nickel producers in Indonesia. The objective is to identify differentiation processes such as enrichment, depletion, and the localization of REE in lateritic outcrops. Apart from geochemical analyses, susceptibility measurements were also carried out to test whether the magnetic susceptibility values correlated with the contents of several critical metals, as reported in a review by **Santoro et al. (2022)**.

2. Materials and Methods

1.1. Geological Setting

Tectonic conditions on Sulawesi Island are complex and resulted from a highly complicated tectonic system during the Late Cretaceous and Early Tertiary in which the Philippine, Australian, and Eurasian plates were in interaction (**Hall and Wilson, 2000; Hall, 2012**). As a result of this tectonic process, Sulawesi Island possesses extremely complex geological features that are represented in its distinctive K-shaped form (**see Figure 1a**). The island's uniqueness leads to metallogonic richness (nickel laterite deposit), particularly the abundance of ultramafic rocks as the source rock for the formation processes (**Kadarusman et al., 2004; Surono, 2013; Choi et al., 2021**). Peridotite (lherzolite, harzburgite, and dunite), gabbro, microgabbro, pyroxenite, diabase, serpentinite, and pelagic make up the group of oceanic crustal rocks known as ophiolite (**see Figure 1b**). This study area in South Konawe Regency of Southeast Sulawesi Province is located in a mafic-ultramafic ophiolite strip that is under the control of a localised fault system (**Surono, 2013; Zhang et al., 2020**). Based on the onsite geological observations in the study area (**see Figure 1c**), the outcrops are located under the layers of

Figure 2: The studied lateritic outcrop showing profiles A (left, red triangle) and B (right, blue triangle).
The bottom parts of the profiles only show yellow limonite and its transition zone towards saprolite.

the Langkowala, Boepinang, and Eemoiko formations, also known as "Molasa Sulawesi" (**Surono, 2013**), which overlie the ultramafic complex. In this part of Sulawesi, weathering of ultramafic rocks produces Ni laterite deposits. The bedrock was found to be peridotite (see **Figure 1d**) and serpentinite (see **Figure 1e**).

1.2. Materials

Sixteen samples were collected for examination from two profiles on the same outcrop. The two profiles (termed A and B, respectively) are located about 3 metres from each other. The outcrop is about 240 cm thick in depth, and samples were taken at an interval of 30 cm in each profile to obtain detailed changes in both magnetic susceptibility as well as pedogenic processes. The profiles cover the following layers (from top to bottom): red limonite, yellow limonite, and saprolite (**see Figure 2**). The profiles were carefully scraped to expose a fresh surface layer. Sampling was carried out by taking about 3 kg of material from each position. The samples were then air dried to remove the remaining water content. The dried samples were ground with a mortar and pestle. Following that of **Yang et al. (2017)**, **Yang et al. (2019)**, **Ouyang et al. (2020)**, and **Wang and Zeng (2022)**, ground samples were then sieved with a 200-mesh-size sieve (74 μm) to obtain grain sizes that are suitable for XRF analyses. Some of the sieved samples were placed in an 8 cm³ standard cylindrical plastic holder for magnetic susceptibility analyses. Other samples were prepared for geochemical analyses by pressing them into pellets that are 4 cm in diameter and 4 mm in thickness.

1.3. Methods

Magnetic susceptibility analyses were carried out using a Bartington MS-3 magnetic susceptibility system

(**Bartington Ltd., Oxford, UK**) that uses an MS-3 metre and MS-2B dual frequency sensors. The parameters measured are mass-specific magnetic susceptibility at low (470 Hz) and high (4700 Hz) frequencies, referred to as χ_{LF} and χ_{HF}, respectively. The third parameter, $\chi_{FD\%}$ is calculated using the equation (**Dearing, 1999**; **Tamuntuan et al., 2015**). Parameters χ_{LF} and χ_{HF} indicate the quantity of magnetic minerals, while $\chi_{FD\%}$ indicates the contribution of superparamagnetic (SP) grains. For magnetite (Fe_3O_4), which is the most common magnetic mineral in nature, SP grains are grains that are < 30 nm. SP grains are similar paramagnetic grains with much higher magnetic susceptibility (**Dearing, 1999**). Low $\chi_{FD\%}$ values indicate the absence or small contribution of SP grains, while high $\chi_{FD\%}$ values indicate a higher contribution of SP grains (**Dearing, 1999**). Magnetic analyses were performed at the Institut Teknologi Bandung's Laboratory of Characterization and Modeling of Physical Rock Properties. The geochemical analyses were carried out using EDAX Orbis Micro X-ray Fluorescence, or EDXRF, equipment (**EDAX Ltd., Mahwah, NJ, USA**) to generate chemical maps of the samples. These analyses were conducted at the Research Center for Nanoscience and Nanotechnology (RCNN), Institut Teknologi Bandung. The results of these analyses are the concentrations of major oxides, transition metals (Ni, Co, Sc, Cr, and V), and REEs (Sc, La, Ce, Nd, Gd, and Ho). This type of XRF, termed μ-XRF, has a spatial resolution diameter that is many orders of magnitude smaller than conventional XRF (**Bran-Anleu et al., 2018; Sharps et al., 2021**).

3. Results

Table 1 shows the values of the χ_{LF} and $\chi_{FD\%}$ measurements of the two profiles. The χ_{LF} and $\chi_{FD\%}$ values

Table 1: Results of magnetic susceptibility measurements on samples from profiles A and B

Depth (cm)	PROFILE A			PROFILE B		
	$\chi_{LF\,(\times 10^{-8}\,m^3/kg)}$	$\chi_{FD\%}$	Ratio ($\chi_{LF}/\chi_{FD\%}$)	$\chi_{LF\,(\times 10^{-8}\,m^3/kg)}$	$\chi_{FD\%}$	Ratio ($\chi_{LF}/\chi_{FD\%}$)
30	1,331.77 ± 0.23	5.05	263.72	1,317.6 ± 0.31	7.73	170.45
60	1,075.68 ± 0.56	5.73	187.73	1,321.18 ± 0.15	6.91	191.20
90	1,238.65 ± 0.49	5.47	226.44	1,395.96 ± 0.29	5.09	274.26
120	**1,127.41 ± 0.38**	**4.06**	277.68	**1,129.02 ± 0.37**	**5.59**	201.97
150	**942.89 ± 0.18**	**3.77**	250.10	**878.27 ± 0.19**	**1.69**	519.69
180	1,148.30 ± 0,10	2.06	557.43	299.69 ± 0.19	3.52	85.14
210	322.80 ± 0.22	1.9	169.89	184.28 ± 0.45	0.96	191.96
240	264.15 ± 0.69	1.8	146.75	257.60 ± 0.38	0.71	362.82
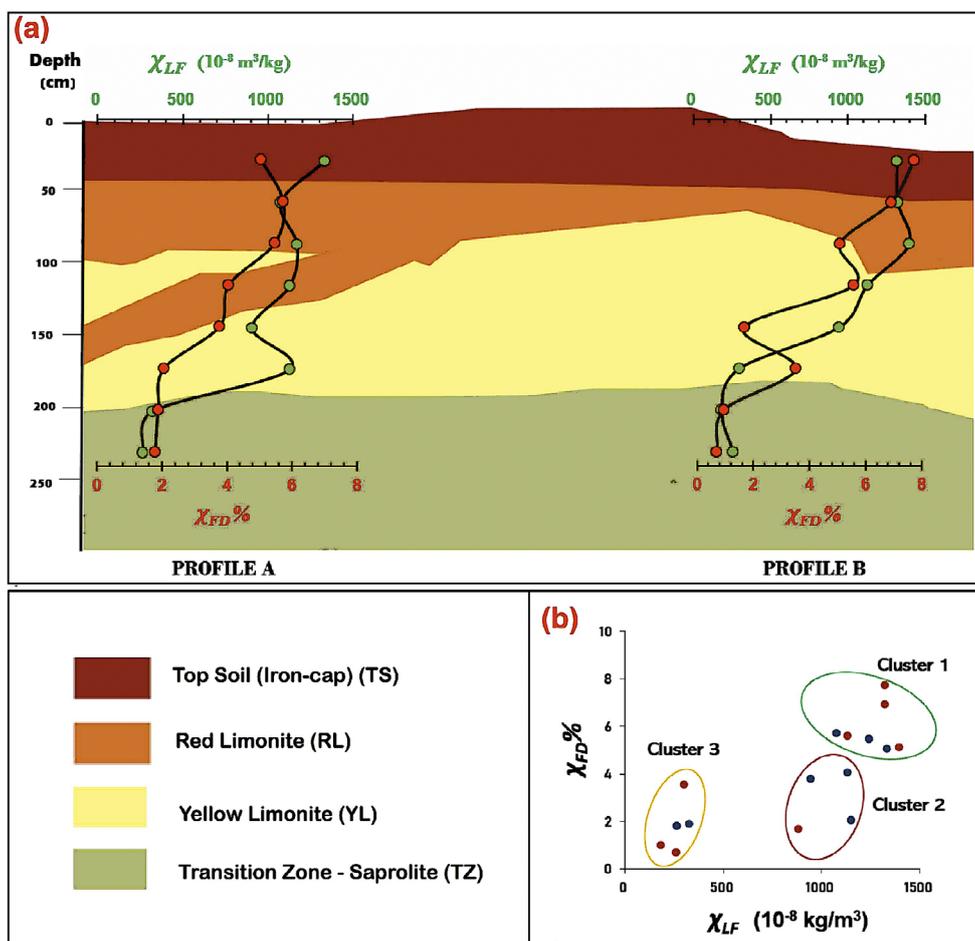
Figure 3: Profiles of χ_{LF} versus depth at both profiles A and B (a) and the plots of $\chi_{FD\%}$ versus χ_{LF} showing three different clusters (b). The red and blue dots in (b) represent data for profiles A and B respectively. A detailed explanation is given in the text.

changed as they increased from the bottom layer to the top. In each profile, it is clear that there is a change in χ_{LF} and $\chi_{FD\%}$ values at a depth of 120–150 cm. For more details, the depth profile for the ratio can be seen in **Figure 3a**. **Table 1** shows that the values of $\chi_{LF}/\chi_{FD\%}$ ratio could be grouped into 3 clusters, which can be seen more clearly in **Figure 3b**, namely: cluster 1 has a high χ_{LF} value with a high $\chi_{FD\%}$ ($\chi_{FD\%} \geq 5\%$); cluster 2 has a high χ_{LF} value with a low $\chi_{FD\%}$ percentage $\chi_{FD\%} < 5\%$; and cluster 3 has low χ_{LF} and $\chi_{FD\%}$ values.

Table 2 shows the results of the geochemical analysis. Certain oxides have increased concentrations from the bottom up, namely Fe, Cr, and Al; there are oxides that experience concentration depletion from the bottom up, namely Si and Mg; and there are also other oxides that do not change significantly with depth, such as Mn.

Table 2: The concentration of the selected major oxide and critical metals on the two profiles

PROFILE A														
DEPTH	Major Oxide (wt%)						Critical Metals and REEs (in mg/kg unit)							
	Fe_2O_3	SiO_2	Cr_2O_3	MgO	Al_2O_3	MnO	Ni	Co	V	Ti	Cr	Sc	Ce	Nd	Ho	La
A-30	43.37	37.98	1.58	1.30	8.87	0.69	6360	4660	1160	4690	17740	2150	2860	330	11750	8930
A-60	36.85	42.26	1.08	1.69	10.13	0.69	13530	10270	1700	3530	12630	1290	3010	3590	13020	7250
A-90	40.31	39.10	1.14	1.19	9.31	0.85	13910	8810	1070	3370	13230	2160	2860	1400	13140	9020
A-120	51.26	29.87	1.55	0.91	9.72	0.72	10980	6790	1230	3740	16360	1600	2590	2960	18110	8960
A-150	41.06	38.00	1.36	3.07	9.52	0.66	15900	5680	1500	3640	15210	1540	5150	3150	14750	8250
A-180	39.79	38.42	1.14	3.34	9.62	0.77	11470	4610	1240	3910	12930	1330	4390	4250	17750	7910
A-210	32.71	37.67	1.04	11.98	6.12	0.36	26540	2300	660	3490	10360	900	1470	3710	19380	8040
A-240	23.37	47.20	0.89	16.55	3.25	0.85	39680	4610	930	970	11090	1430	1590	5980	21260	6890
PROFILE B														
DEPTH	Major Oxide (wt %)						Critical Metals and REEs (in mg/kg unit)							
	Fe_2O_3	SiO_2	Cr_2O_3	MgO	Al_2O_3	MnO	Ni	Co	V	Ti	Cr	Sc	Ce	Nd	Ho	La
B-30	46.15	36.04	2.74	0.00	7.69	0.64	7430	4250	1330	5180	29990	1940	4160	4170	7350	10790
B-60	43.64	37.62	1.21	1.68	7.42	0.59	13580	5340	970	3790	13720	1970	5610	2750	7160	10920
B-90	41.46	40.60	1.92	2.64	6.02	0.63	16120	7910	1770	2630	21770	2310	3030	3110	12640	10640
B-120	39.31	41.91	1.30	3.51	7.14	0.72	20960	7630	1270	3940	14820	1750	2140	2590	8830	10810
B-150	29.39	45.30	1.48	6.83	6.53	0.53	24710	5140	1260	3310	18030	1160	1190	3910	12610	5560
B-180	23.76	46.22	1.26	13.63	5.16	0.46	29380	4750	1230	3150	15530	1020	3000	5660	11460	7420
B-210	17.93	52.89	1.03	15.30	3.01	0.52	40010	4130	800	1120	13850	1700	2250	8370	13850	5730
B-240	19.04	52.03	0.53	17.12	3.68	0.45	41240	5880	1160	1810	6980	1160	1470	6860	18180	7150

In addition, **Table 2** also shows the concentration values of critical metals and REEs. Certain metals have increased in concentration from the bottom up, namely Sc, La, Cr, and Ti; there is also a group of metals that experience concentration depletion from the bottom up, namely Ni, Ho, and Nd; and there are also other groups that do not experience significant changes with depth, such as Ce, Co, and V. For more details, see **Figure 4**.

4. Discussion

The results shown in **Table 1** and **Figure 3** regarding the variations in χ_{LF} and $\chi_{FD\%}$ values in laterite profiles are influenced by variations in magnetic minerals, especially Fe minerals, which are formed during the pedogenesis process. From the results of cluster division (see **Figure 3b**), the characteristics of cluster 1 are indicated due to the presence of ultrafine superparamagnetic minerals produced during the pedogenesis process, which are formed in the uppermost layer of laterite (the red limonite zone). Cluster 2 occurs because magnetite SP grains are unstable, so they experience oxidation processes and change into hematite and goethite. In both profiles (A and B), cluster 2 is found in the yellow limonite layer. Cluster 3 has low χ_{LF} and $\chi_{FD\%}$ in the transition zone between yellow limonite and saprolite. This cluster forms because the layer above the transition zone is stable, so mobilisation of Fe minerals in the lower layer is

minimal but labile minerals are added. Generally, these labile minerals are diamagnetic, including Si and Mg. As discussed by **Szuszkiewicz et al. (2021)**, iron oxide plays an important role in pedogenic processes, including the transfer and transformation of iron (Fe) minerals in the soil.

During the pedogenesis process, not only the mobilisation of Fe minerals occurs but also changes in critical metal concentrations, which result in the emergence of patterns of enrichment, depletion, and localization. The enrichment pattern shows an increase in the concentration of major oxides and minerals from the bottom layer up. This pattern has similarities with the laterite pedogenesis process, where there are several metal elements and REE that experience enrichment near the surface, or the same with the abundance of Fe minerals. One of the REE metals that has experienced enrichment with a clear trend is Sc (**Figure 4a**). The relationship between the presences of Sc and Fe has been reported in earlier studies (**Chassé et al., 2017**; **Putzolu et al., 2019**). As reported by **Teittler et al. (2019)**, **Ulrich et al. (2019)**, and **Santoro et al. (2022)**, the highest Sc content is in the red limonite and limonite transition zones, and generally, this zone consists of magnetic minerals (goethite and hematite) (**Choi et al., 2021**).

During the pedogenesis process in laterite cases in this study, several factors might have occurred that affected the enrichment of critical metals at the top, espe-
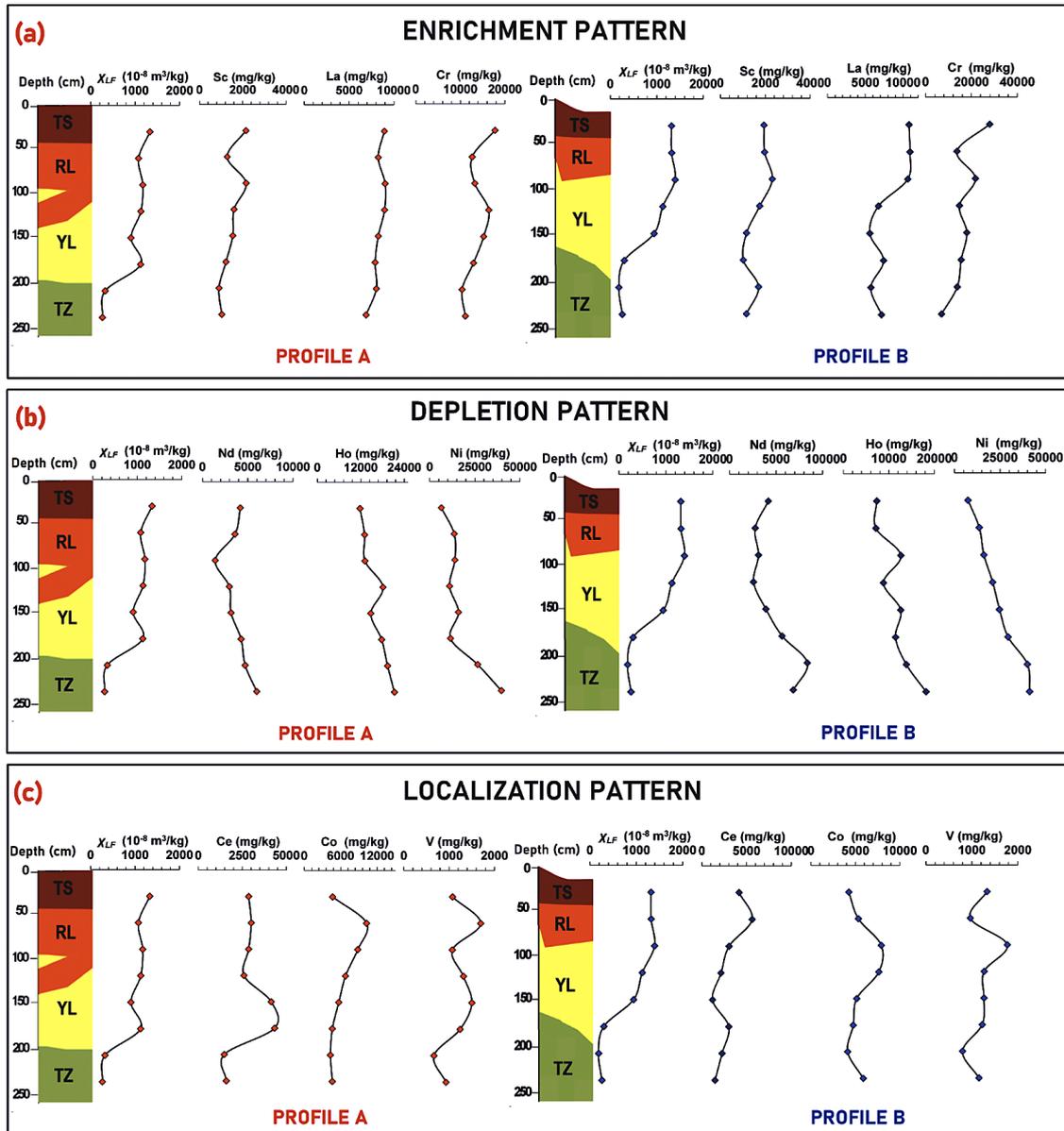
Figure 4: Patterns of REE variation on the lateritic soil in this study: (a) enrichment patterns; (b) depletion patterns; and (c) localised patterns. TS represents topsoil, RL represents red limonite, YL represents yellow limonite, and TZ represents transition zone to saprolite.

cially Sc: (1) a weathering time scale that allows Sc capture by Fe oxide; (2) Sc has increased in the upper and lower limonite zones; and (3) Sc and several other REEs have the same pattern as the pedogenesis process during the transformation of magnetite SP grains to goethite and hematite. When there is a lot of weathering, the limonite zone forms because water keeps moving downward, carrying unstable (highly mobile) elements and leaving stable (not mobile) elements in the uppermost horizon. As long as the water supply stays the same, this pedogenesis process will lead to in situ enrichment because Fe, Al, Cr, and Ti are more stable or immobile and will stay in the top layer (**Choi et al., 2021**).

The depletion pattern is the opposite of enrichment during the pedogenesis process. This pattern is associ-

ated with the presence of labile minerals (minerals that readily mobilize). One of the minerals found in profiles A and B experiencing depletion is Ni. The maximum concentration of Ni is found in the saprolite zone (see **Figure 4b**), similar to that reported in Brazil (**Putzolu et al., 2021**), Central Sulawesi (**Choi et al., 2021**), and New Caledonia (**Teittler et al., 2019**). **Figure 5** shows high SiO_2 and MgO contents above the bedrock. Earlier, based on their study in Morowali, Sulawesi, **Choi et al. (2021)** concluded that high Ni content in the bottom layer occurred when Ni came into contact with dissolved labile minerals (Si, Mg) and formed garnierite ($H_2O(Mg, Ni)_3Si_4O_{10}(OH)_2$).

The localization pattern does not show a trend of significant concentration changes in mineral groups from
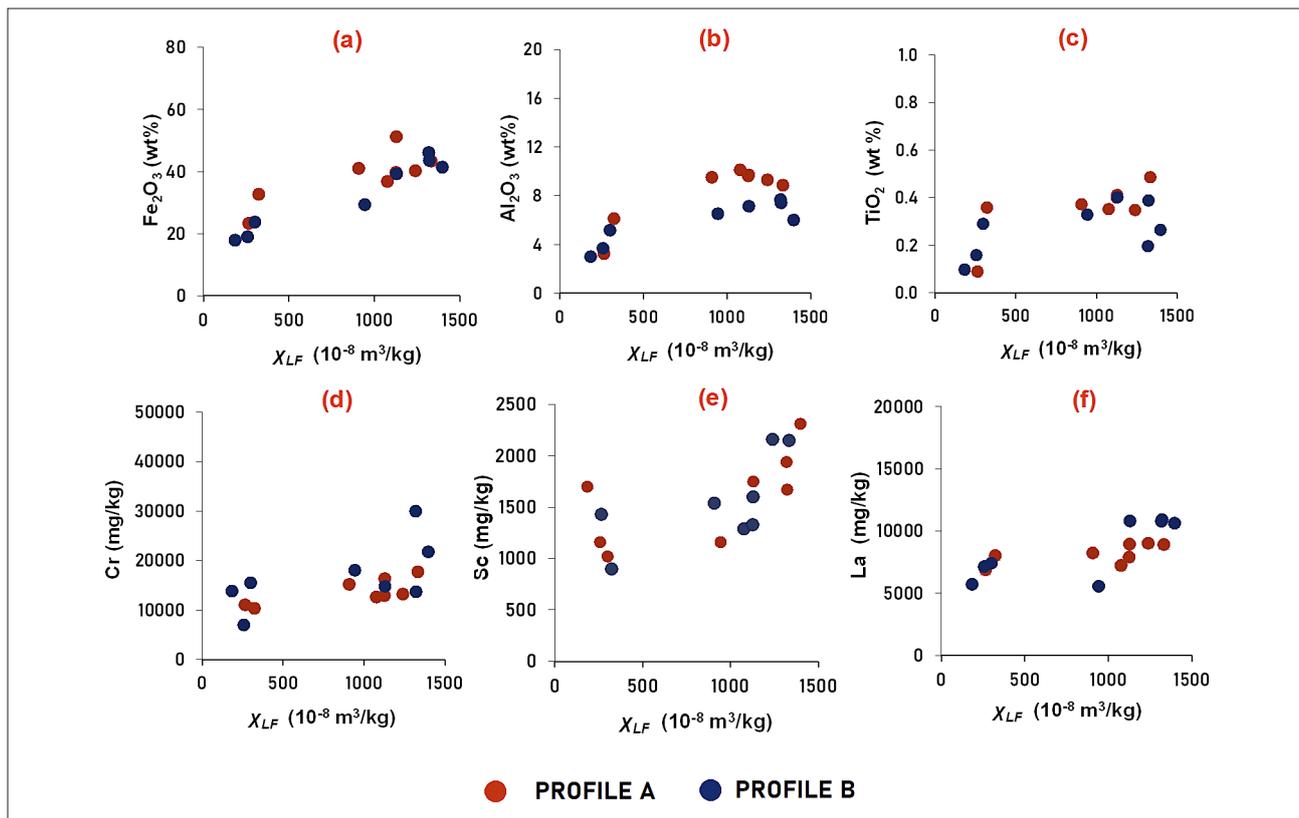
Figure 5: Correlation between χ_{LF} and main oxides, critical metals, and REE in lateritic soils in this study. (a) Fe_2O_3 versus χ_{LF}, (b) Al_2O_3 versus χ_{LF}, (c) Sc versus χ_{LF}, (d) La versus χ_{LF}, (e) Ti versus χ_{LF}, (f) Cr versus χ_{LF}, and (g) Ni versus SiO_2.
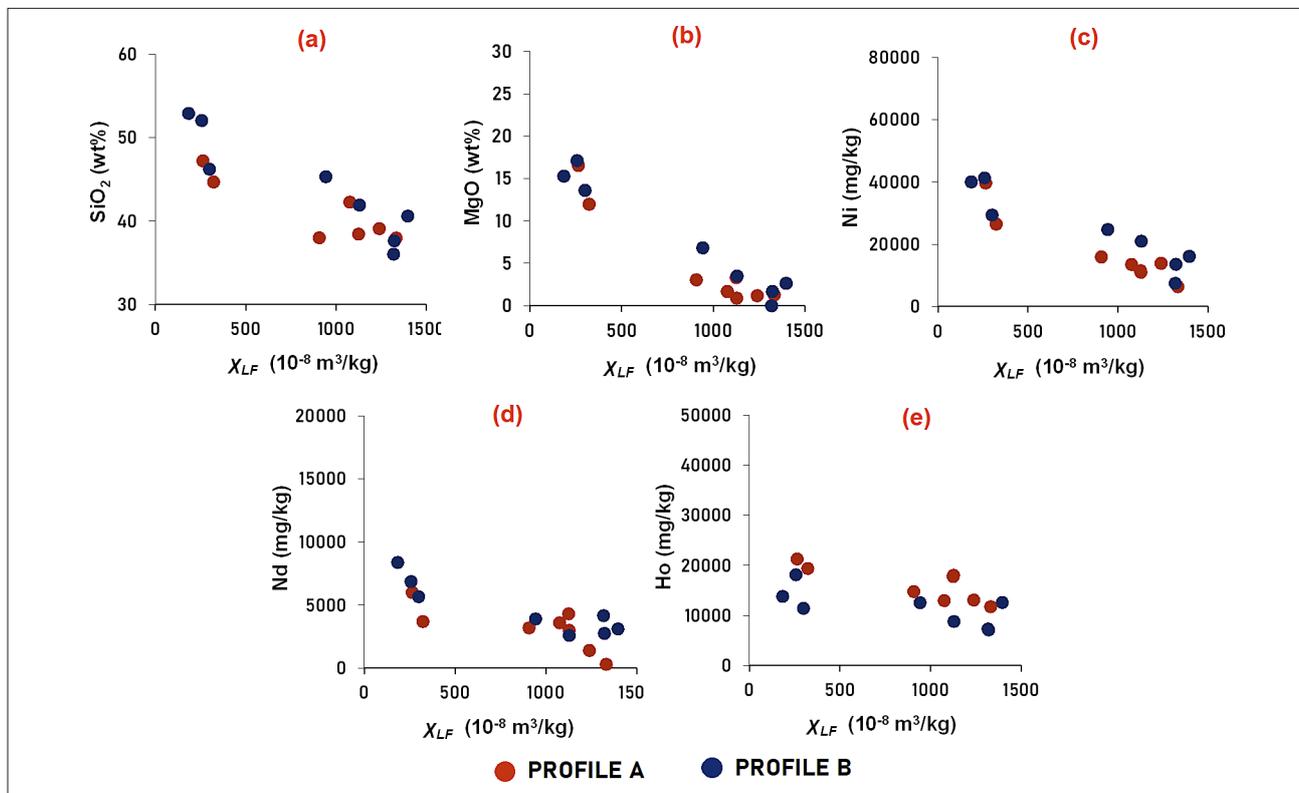
Figure 6: Plots of the negative correlation between χ_{LF}, major oxides, critical metals, and REE in this study. Correlation between χ_{LF} and main oxides, critical metals, and REE in lateritic soils in this study. (a) Ni versus χ_{LF}, (b) MgO versus χ_{LF}, (c) SiO_2 versus χ_{LF}, (d) Nd versus χ_{LF}, and (e) Ho versus χ_{LF}.

Table 3: Pearson's correlation coefficient (r) between χ_{LF} values and concentrations of major elements and critical metals in this study. Values of $|r| > 0.622$ are marked in bold typeface indicating significant positive (or negative) correlations. See text for details.

Parameters	Major Oxide (Fe$_2$O$_3$, SiO$_2$, MgO, MnO, Al$_2$O$_3$)					Critical Metals and REEs (Ni, Co, V. Ti, Cr, Sc, Ce, Nd, Ho, La)									
PROFILE A															
	Fe$_2$O$_3$	SiO$_2$	MgO	MnO	Al$_2$O$_3$	Ni	Co	V	Ti	Cr	Sc	Ce	Nd	Ho	La
χ_{LF}	**0.82**	**-0.77**	**-0.96**	0.56	**0.87**	**-0.95**	0.42	0.57	**0.75**	**0.76**	**0.77**	**0.66**	**-0.66**	**-0.78**	**0.78**
Fe$_2$O$_3$		**-0.97**	**-0.90**	0.40	**0.79**	**-0.89**	0.30	0.48	**0.79**	**0.79**	0.59	0.50	**-0.68**	-0.51	**0.87**
SiO$_2$			0.86	-0.47	**-0.73**	0.82	-0.37	-0.62	**-0.67**	**-0.72**	-0.45	-0.53	**0.63**	0.41	**-0.74**
MgO				-0.51	**-0.92**	**0.96**	-0.52	**-0.64**	**-0.80**	**-0.71**	**-0.70**	**-0.67**	0.78	0.78	-0.85
MnO					**0.65**	-0.52	-0.03	0.59	0.35	0.37	0.15	**0.94**	-0.19	-0.21	0.06
Al$_2$O$_3$						**-0.95**	0.30	0.55	**0.89**	0.57	0.53	**0.80**	**-0.64**	**-0.72**	**0.71**
Ni							-0.32	-0.51	**-0.91**	**-0.74**	**-0.67**	**-0.65**	**0.65**	**0.75**	**-0.84**
Co								0.62	0.08	0.02	0.30	0.13	**-0.65**	-0.53	0.40
V									0.26	0.39	0.17	**0.67**	-0.38	-0.49	0.23
Ti										**0.63**	**0.75**	0.30	-0.41	0.62	0.47
Cr											**0.75**	0.43	-0.39	-0.57	**0.69**
Sc												0.30	**-0.69**	**-0.77**	**0.80**
Ce													-0.41	-0.46	0.26
Nd														0.62	**-0.81**
Ho															-0.70
PROFILE B															
Parameters	Major Oxide (Fe$_2$O$_3$, SiO$_2$, MgO, MnO, Al$_2$O$_3$)					Critical Metals and REEs (Ni, Co, V, Ti, Cr, Sc, Ce, Nd, Ho, La)									
	Fe$_2$O$_3$	SiO$_2$	MgO	MnO	Al$_2$O$_3$	Ni	Co	V	Ti	Cr	Sc	Ce	Nd	Ho	La
χ_{LF}	**0.97**	**-0.92**	**-0.98**	0.58	**0.87**	**-0.93**	0.44	0.54	**0.72**	0.62	**0.67**	0.52	**-0.90**	**-0.70**	**0.70**
Fe$_2$O$_3$		**-0.98**	**-0.98**	0.56	**0.90**	**-0.98**	0.35	0.48	**0.81**	**0.66**	0.66	0.65	-0.88	-0.81	0.77
SiO$_2$			0.96	-0.45	**-0.93**	0.99	-0.21	-0.44	**-0.88**	**-0.70**	-0.54	**-0.72**	0.85	0.86	-0.79
MgO				-0.55	**-0.94**	**0.96**	-0.38	-0.52	**-0.82**	**-0.64**	-0.57	-0.54	**0.94**	0.78	**-0.68**
MnO					0.35	-0.49	0.41	0.18	0.34	0.43	**0.70**	0.12	-0.49	-0.57	0.10
Al$_2$O$_3$						**-0.92**	0.17	0.37	**0.93**	0.58	0.27	0.55	**-0.89**	**-0.81**	0.59
Ni							-0.19	-0.47	**-0.87**	**-0.77**	-0.58	**-0.67**	**0.83**	**0.84**	**-0.77**
Co								**0.65**	0.00	-0.11	0.42	-0.16	-0.57	0.05	0.16
V									0.30	0.51	0.43	-0.07	-0.54	-0.03	0.41
Ti										**0.66**	0.56	0.41	-0.40	**0.67**	**0.83**
Cr											0.56	0.35	-0.39	-0.58	0.51
Sc												0.41	-0.39	-0.39	0.62
Ce													-0.40	**-0.73**	**0.83**
Nd														0.67	-0.52
Ho															-0.53

the bottom layer up during the pedogenesis process. Critical metals with localization patterns found in profiles A and B are Co, Ce, and V, all three of which have a similar pattern of maximum concentrations in the limonite zone and minimum concentrations in the saprolite zone (see **Figure 4c**). This is supported by the results of studies in Southeast Cameroon (**Ndjigui et al., 2009**) and North Cameroon (**Sababa et al., 2021**) that indicate negative Ce concentrations are located in the saprolite zone. The minimum Ce concentration in the saprolite zone is thought to be due to the decomposition of the primary phase of iron oxide (magnetite) (**Ndjigui et al., 2009**). The decomposition of this iron oxide affects the levels of magnetic minerals, so that the χ_{LF} value is small in the saprolite zone. The pattern of maximum and minimum Co concentrations is supported by the study of **Putzolu et al. (2018)** in Wingellina (Western Australia), which found that the highest Co concentration was in the limonite zone and decreased in concentration in the saprolite zone. Studying the granitic weathering materials

from North Cameroon, **Sababa et al. (2021)** reported that the maximum V concentration was in weathered rock fragments termed the iron duricrust horizon.

Several elements detected in profiles A and B have a correlation with the presence of other elements, so in studying certain REE characteristics, it is necessary to look at the positive and negative correlations between several elements. **Table 3** shows the Pearson correlation coefficients (r) between χ_{LF}, the concentration of major elements, and critical metals. Since each profile has only 8 samples, i.e., $n = 8$, the critical value for r at the 0.05 level of significance is 0.622 (**Nino-Zarazua, 2012**). In **Table 3**, r values that are higher than 0.622 (or lower than -0.622) are marked in bold typeface, indicating significant positive (or negative) correlations between the parameters. Significant positive correlations were found between the values of χ_{LF} and Fe_2O_3, Al_2O_3, Ti, Cr, La, and Sc. These correlations are more clearly seen in **Figure 5**. As has been shown and reported by **Teitler et al. (2022)**, Al_2O_3 correlates well with Sc. On the other hand, Sc is in conflict with the abundance of MgO and SiO_2 concentrations. SiO_2 and MgO levels decrease from the bedrock to near the surface. Moreover, the concentration of χ_{LF} was negatively correlated with the presence of Ni, MgO, SiO_2, Ho, and Nd (see **Figure 6**). The abundance of magnetic minerals during the pedogenesis process has a significant influence on the presence of REE in lateritic soils. From the results discussed, it was found that magnetic parameters can be used as a proxy to observe the pedogenesis process in laterite; besides that, they can be used as an indicator of the presence of some metals, such as high Ni concentration associated with low χ_{LF}, and low Sc concentration associated with high χ_{LF}.

5. Conclusion

The pedogenesis process of lateritic soils is controlled by the abundance of iron oxide minerals, which are characterised by an increase in the value of magnetic susceptibility from the source rock to the upper profile of lateritic nickel deposits. During the pedogenesis process, the magnetite mineral changes grain size from coarse to fine, as shown by changes in $\chi_{FD\%}$ values that are low at the bottom and high at the top. The magnetite SP grains in the uppermost zone have changed into iron oxide minerals (hematite and goethite). Based on the studies conducted, there are three patterns of changes in critical metal concentrations during the pedogenesis process: 1) The enrichment pattern has the same pattern as the pedogenesis process (increasing concentration from the bottom layer up), as seen in the metal concentration patterns of Sc, La, Cr, and Ti; 2) the depletion pattern shows decreased concentration from the bottom layer up due to remobilization with labile minerals (Mg, Si) and deposits in the bottom layer, as seen in the concentration pattern of Ni, Nd, and Ho; and 3) the localization pattern, in which high concentrations of certain metals (Co, Ce, and

V) occurred at a certain depth. From the results of geochemical and magnetic susceptibility tests, it is known that the concentration of critical metals in lateritic soils depends on the amount of magnetic minerals. The increase in susceptibility value indicates an increase in magnetic mineral concentration. This can be seen in the increase in the concentration of the critical metals Sc, Co, and La in the limonite zone, which has a positive correlation with the χ_{LF} value. However, it is inversely proportional to Ni, Nd, and Ho, which are negatively correlated with χ_{LF}. Thus, the rock magnetism method can be considered a proxy to see the pattern of the presence of critical metals in the laterite profile.

6. References

Aiglsperger, T., Proenza, J.A., Lewis, J.F., Labrador, M., Svotjka, M., Rojas-Purón, A., Longo, F., and Ďurišová, J. (2016): Critical metals (REE, Sc, PGE) in Ni laterites from Cuba and the Dominican Republic, Ore Geology Reviews, 73, 127-147. https://doi.org/10.1016/j.oregeorev.2015.10.010.

Ananthapadmanabha, L., Shankar, R., and Sandeep, K. (2014): Rock magnetic properties of lateritic soil profiles from southern India: Evidence for pedogenic processes. Journal of Applied Geophysics, 111, 203-210. https://doi.org/10.1016/j.jappgeo.2014.10.009.

Balaram, V. (2019): Rare earth elements: A review of applications, occurrence, exploration, analysis, recycling, and environmental impact. Geoscience Frontiers, 10(4), 1285-1303. doi: https://doi.org/10.1016/j.gsf.2018.12.005.

Balaram, V. (2022): Rare Earth Element deposits: sources, and exploration strategies. Journal of Society India, 98, 1210–1216 . https://doi.org/10.1007/s12594-022-2154-3

Batapola, N.M., Dushyantha, N.P., Premasiri, H.M.R., Abeysinghe, A.M.K.B., Rohitha, L.P.S., Ratnayake, N.P., Dissanayake, D.M.D.O.K., Ilankoon, I.M.S.K., and Dharmaratne P.G.R. (2020): A comparison of global rare earth element (REE) resources and their mineralogy with REE prospects in Sri Lanka. Journal of Asian Earth Sciences, 200, 104475. https://doi.org/10.1016/j.jseaes.2020.104475.

Berger, A., Janots, E., Gnos, E., Frei, R., and Bernier, F. (2014): Rare earth element mineralogy and geochemistry in a laterite profile from Madagascar. Applied Geochemistry, 41, 218-228. https://doi.org/10.1016/j.apgeochem.2013.12.013.

Botelho Junior, A. B., Espinosa, D. C. R., Vaughan, J., and Tenório, J.A.S. (2021): Recovery of scandium from various sources: A critical review of the state of the art and prospects. Minerals Engineering, 172, 107148, https://doi.org/10.1016/j.mineng.2021.107148.

Bran-Anleu, P., Caruso, F., Wangler, T., Pomjakushina, E., and Flatt, R.J. (2018): Standard and sample preparation for the micro XRF quantification of chlorides in hardened cement pastes. Microchemical Journal, 141, 382–387. https://doi.org/10.1016/j.microc.2018.05.040.

Chassé, M., Griffin, W., O'Reilly, S. Y., and Calas, G. (2017): Scandium speciation in a world-class lateritic deposit. Geochemical Perspectives Letters, 3(2), 105–114. https://doi.org/10.7185/geochemlet.1711.

Choi, Y., Lee, I., and Moon, I. (2021): Geochemical and mineralogical characteristics of garnierite from the Morowali Ni-Laterite deposit in Sulawesi, Indonesia. Frontier Earth Science, 9, 761748. doi: https://doi.org/10.3389/feart.2021.761748.

Dearing, J. (1999): Environmental magnetic susceptibility: Using the bartington MS2 system. Chi Publishing, Keniloworth.

Farrokhpay, S., Cathelineau, M., Blancher, S.B., Laugier, O., and Filippov, L. (2019): Characterization of Weda Bay nickel laterite ore from Indonesia. Journal of Geochemical Exploration, 196, 270-281. https://doi.org/10.1016/j.gexplo.2018.11.002.

Gibaga, C. R. L., Samaniego, J.O., Tanciongco, A.M., Quierrez, R.N.M., Montanao, M.O., Gervasio, J.H.C., Reyes, R.C.G., and Peralta, M.J.V. (2022): The rare earth element (REE) potential of the Philippines, Journal of Geochemical Exploration, 242, 107082. https://doi.org/10.1016/j.gexplo.2022.107082.

Goodenough, K.M., Schilling, J., Jonsson, E., Kalvig, P., Charles, N., Tuduri, J., Deady, E.A., Sadeghi, Schiellerup, M. H., Müller, A., Bertrand, G., Arvanitidis, N., Eliopoulos, D.G. Shaw, R.A., Thrane, K., and Keulen, N. (2016): Europe's rare earth element resource potential: An overview of REE metallogenetic provinces and their geodynamic setting. Ore Geology Reviews, 72, 838–856. http://dx.doi.org/10.1016/j.oregeorev.2015.09.019.

Hall, R., and Wilson, M.E.J. (2000): Neogene sutures in eastern Indonesia. Journal of Asian Earth Sciences, 18, 781-808. https://doi.org/10.1016/S1367-9120(00)00040-7.

Hall, R. (2012): Late Jurassic–Cenozoic reconstructions of the Indonesian region and the Indian Ocean. Tectonophysics, 570–571, 1-41. https://doi.org/10.1016/j.tecto.2012.04.021.

Hamdan, A.M., Bijaksana, S. Tjoa, A., Dahrin, D., Fajar, S.J., Kirana, K.H. (2020): Use and validation of magnetic properties for differentiating nickel hyperaccumulators and non-nickel hyperaccumulators in ultramafic regions. Journal of Geochemical Exploration, 216, 106581. https://doi.org/10.1016/j.gexplo.2020.106581.

Hayes, S.M., and McCullough, E.A. (2018): Critical minerals: A review of elemental trends in comprehensive criticality studies. Resources Policy. 59, 192-199. https://doi.org/10.1016/j.resourpol.2018.06.015.

Ilankoon, I.M.S.J., Dushyantha, N.P., Mancheri, N., Edirisinghe, P.M., Neethling, S.J., Ratnayake, N.P., Rohitha, L.P.S., Dissanayake, D.M.D.O.K., Premasiri, H.M.R., Abeysinghe, A.M.K.B, Dharmaratne, P.G.R., and Batapola, N.M. (2022): Constraints to rare earth elements supply diversification: Evidence from an industry survey, Journal

of Cleaner Production, 331, 129932. https://doi.org/10.1016/j.jclepro.2021.129932.

Kadarusman, A., Miyashita, S., Maruyama, S., Parkinson, C. D., and Ishikawa, A. (2004): Petrology, Geochemistry and Paleogeographic Reconstruction of the East Sulawesi Ophiolite, Indonesia. Tectonophysics, 392, 55–83. doi:10.1016/j.tecto.2004.04.008.

Maulana, A., Sanematsu, K., and Sakakibara, M. (2016): An overview on the Possibility of Scandium and REE occurence in Sulawesi, Indonesia, Indonesian Journal on Geoscience, 3, 139-147. https://doi.org/10.17014/ijog.3.2.139-147.

Ndjigui, P.D., Bilong, P., Bitom, D. (2009): Negative cerium anomalies in the saprolite zone of serpentinite lateritic profiles in the Lomié ultramafic complex, South-East Cameroon. Journal of African Earth Sciences, 53, 56-69. https://doi.org/10.1016/j.jafrearsci.2008.09.002.

Nino-Zarazua, M. (2012): Quantitative analyses in social sciences: A brief introduction for non-economists, SRRN Electronic Journal. http://dx.doi.org/10.2139/ssrn.2066508.

Olivetti, E.A., Ceder, G., Gaustad, G.G., and Fu, X. (2017): Lithium-ion battery supply chain considerations: analysis of potential bottlenecks in critical metals, Joule, 1, 229-243. https://doi.org/10.1016/j.joule.2017.08.019.

Ouyang, T., Li, M., Guo, Y., Peng, S.,He, C., and Zhu, Z. (2020): Magnetic difference between deep and surfaces oil within an agricultural area insouthern China: Implications formagnetic mineral transformation during pedogenic process under subtropical climate. Earth and Space Science, 7, e2019EA001070. https://doi.org/10.1029/2019EA001070.

PSDMBP. (2019): Potensi Logam Tanah Jarang di Indonesia (Rare Earth Metals Potentials in Indonesia). Pusat Sumber Daya Mineral, Batubara dan Panas Bumi, Kementerian Energi dan Sumber Daya Mineral, (Centre for Mineral Resources, Coal and Geothermal, Ministry of Energy and Mineral Resources), Bandung. (In Indonesian).

Putzolu, F., Balassone, G., Boni, M., Maczurad, M., Mondilo, N., Najorka, J., and Pirajno, F. (2018): Mineralogical association and Ni-Co deportment in the Wingellina oxide-type laterite deposit (Western Australia). Ore Geologi Reviews, 97,21-34. https://doi.org/10.1016/j.oregeorev.2018.05.005.

Putzolu, F., Boni, M., Mondillo, N., Maczurad, M., and Pirajno, F. (2019): Ni-Co enrichment and High-Tech metals geochemistry in the Wingellina Ni-Co oxide-type laterite deposit (Western Australia). Journal of Geochemical Exploration, 196, 282-296. https://doi.org/10.1016/j.gexplo.2018.11.004.

Putzolu, F., Santoro, L., Porto, C., Mondillo, N., Machado, M., De Almeida, B.S., and Herrington, R. (2021): The influence of the magmatic to postmagmatic evolution of the parent rock on the Co deportment in lateritic systems: the example of the Santa Fé Ni-Co deposit (Brazil). Economics Geology, 116: 837–861. https://doi.org/10.5382/econgeo.4819.

Sababa, E., Owona, L.G.E., Temga, J.P., and Ndjigui, P.D. (2021): Petrology of weathering materials developed on granites in Biou area, North-Cameroon: implication for

rare-earth elements (REE) exploration in semi-arid regions. Heliyon, 7, E08581. https://doi.org/10.1016/j.heliyon.2021.e08581.

Safiuddin, L.O., Haris, V., Wirman, R.P., and Bijaksana, S. (2011): A preliminary study of magnetic properties on laterite soils as indicators of pedogenic processess. Latinmag Letter, 1, 1-15.

Santoro, L., Putzolu, F., Mondillo, N., Boni., and Herrington, R. (2022): Trace element geochemistry of iron-(oxy)- hydroxides in Ni(Co)-laterites: Review, new data and implications for ore forming processes. Ore Geology Reviews, 140, 104501. https://doi.org/10.1016/j.oregeorev.2021.104501.

Sharps, M.C., Martinez, M.M., Brandl, M., Lam, T., and Vicenzi, E.P. (2021): A dual beam SEM-based EDS and micro-XRF method for the analysis of large-scale Mesoamerican obsidian tablets, Journal of Archaeological Science: Reports, 35, 102781. https://doi.org/10.1016/j.jasrep.2020.102781.

Simandjuntak, T., Surono, and Sukido (2011): Geological map of the Kolaka quadrangle, Sulawesi, Scale 1: 250.000. Pusat Penelitian dan Pengembangan Geologi, Bandung,

Stratiotou Efstratiadis, V., and Michailidis, N. (2022): Sustainable recovery, recycle of critical metals and rare earth elements from waste electric and electronic equipment (circuits, solar, wind) and their reusability in additive manufacturing applications: a review. Metals, 12, 1-25. https://doi.org/10.3390/met12050794.

Surono. (2013): Geologi Lengan Tenggara Sulawesi. Pusat Survei Geologi Badan Geologi Kementrian Energi dan Sumber Daya Mineral, Bandung.

Szuszkiewicz, M., Grison, H., Petrovský, E., Szuszkiewicz, M.M., Gołuchowska, B., Łukasik, A. (2021): Quantification of pedogenic particles masked by geogenic magnetic fraction. Scientific Reports, 11, 14800. https://doi.org/10.1038/s41598-021-94039-1.

Tamuntuan, G., Bijaksana, S., King J, Russell, J.M., Fauzi, U., Maryunani, K., and Aufa, N., dan Safiuddin, L.O. (2015): Variation of magnetic properties in sediments from Lake Towuti, Indonesia, and its paleoclimatic significance. Palaeogeography, Palaeoclimatology, Palaeoecology, 420, 163–172. https://doi.org/10.1016/j.palaeo.2014.12.008.

Teitler, Y., Cathelineau, M., Ulrich, M., Ambrosi, J.P., Munoz, M., and Sevin, B. (2019): Petrology and geochemistry of scandium in New Caledonian Ni-Co laterites. Journal of Geochemical Exploration, 196. https://doi.org/10.1016/j.gexplo.2018.10.009.

Teitler, Y., Favier, S., Ambrosi, J.-P., Sevin, B., Golfier, F., and Cathelineau, M. (2022): Evaluation of Sc concentrations in Ni-Co laterites using Al as a geochemical proxy. Minerals, 12, 1-22. https://doi.org/10.3390/min12050615.

Ulrich, M., Cathelineau, M., Muñoz, M., Christine-Boiron, M., Teitler, Y., and Karpoff, A.M. (2019): The relative distribution of critical (Sc, REE) and transition metals (Ni, Co, Cr, Mn, V) in some Ni-laterite deposits of New Caledonia. Journal of Geochemical Exploration, 197, 93-113. https://doi.org/10.1016/j.gexplo.2018.11.017.

Wang, L., and Zeng. Z. (2022): The Geochemical Features and Genesis of Ferromanganese Deposits from Caiwei Guyot, Northwestern Pacific Ocean. Journal of Marine Science and Engineering. 10, 1275. https://doi.org/10.3390/jmse10091275

Watari, T., Nansai, K., and Nakajima, K. (2020): Review of critical metal dynamics to 2050 for 48 elements. Resources, Conservation and Recycling, 155, 104669. https://doi.org/10.1016/j.resconrec.2019.104669.

Yang, F., Kong, M., Liu, H., Yu, J., Yang, S., Hao, Z., Zhang, D., and Cen, K. (2017): Discovery of Wolitu Pb-Zn deposit through geochemical prospecting under loess cover in Inner Mongolia, China, Geoscience Frontiers, 8, 951-960. https://doi.org/10.1016/j.gsf.2016.08.007.

Yang, F., Sun, J., Wang, Y., Fu, J., Na, F., Fan, Z., and Hu, Z. (2019): Geology, Geochronology and Geochemistry of Weilasituo Sn-Polymetallic Deposit in Inner Mongolia, China. Minerals, 9, 104. https://doi.org/10.3390/min9020104

Zhang, Y., Qie, J., Wang, X.F. Cui, K., Fu, T., Wang, J., and Qi, W. (2020): Mineralogical Characteristics of the Nickel Laterite, Southeast Ophiolite Belt, Sulawesi Island, Indonesia. Mining, Metallurgy & Exploration 37, 79–91 (2020). https://doi.org/10.1007/s42461-019-00147-y.

SAŽETAK

Pedogeneza lateritnih tala i obogaćivanje kritičnih metala: studija iz jugoistočne Sulawesi, Indonezija

Lateritno tlo je potencijalni izvor metala koji se nazivaju kritični ili strateški metali zbog njihove upotrebe u industrijama visoke tehnologije. Kritični metali uključuju elemente rijetkih zemalja (REE). U ovom istraživanju uzorkovana su dva profila lateritnih izdanaka iz područja proizvodnje nikla u jugoistočnom Sulawesi u Indoneziji, s ciljem definiranja promjene koncentracija kritičnih metala tijekom pedogeneze korištenjem magnetne susceptibilnosti i μ-XRF analiza. Rezultati su ukazali na postojanje tri različita obrasca od donjeg sloja prema gore. Prvi obrazac predstavlja obogaćivanje Sc, La, Cr i Ti. Drugi obrazac predstavljen je sniženjem koncentracija Ni, Nd i Ho. Treći obrazac predstavlja lokalizaciju visokih koncentracija određenih metala na određenoj dubini, kao što su Co, Ce i V. Koncentracija nekih kritičnih metala korelira bilo pozitivno ili negativno s magnetnom susceptibilnosti, što upućuje na to da bi se magnetna susceptibilnost mogla koristiti kao indikator kritičnih koncentracija metala u lateritnom tlu.

Ključne riječi:
Kritični metali, lateritno tlo, pedogeneza, magnetna susceptibilnost, jugoistočni Sulawesi

Author's contribution

Khalil Ibrahim (1) (B.Eng., geophysical engineer with expertise in geophysical exploration) performed the field work and soil sample data collection, magnetic data measurements and processing, provided the data interpretation, composed the original drafting, edited it, and managed the project administration. **Satria Bijaksana (2)** (Ph.D., Rock Magnetism Professor) interpreted rock magnetism data, edited drafts, and held funding acquisition, supervision, and project administration. **Ulvienin Harlianti (3)** (M.Eng., geophysical engineer with expertise in rock magnetism for environmental purposes) provided the data interpretation and editing draft. **Putu Billy Suryanata (4)** (M.Eng., geophysical engineer with expertise in rock magnetism for volcanoes) performed data interpretation. **La Ode Ngkoimani (5)** (Ph.D., Associate Professor, expert on rock magnetism) performed the field work, project administration, and supervision. **Suryawan Asfar (6)** (M.Sc., geologist with expertise in exploration geology) performed the field work and soil sample data collection. **Silvia Jannatul Fajar (7)** (M.Eng., geophysical engineer with expertise in rock magnetism) performed data interpretation and project administration.